medRxiv preprint doi: https://doi.org/10.1101/2024.11.11.24317133; this version posted November 14, 2024. The copyright holder for this preprint (which was not certified by peer review) is the author/funder, who has granted medRxiv a license to display the preprint in perpetuity.
All rights reserved. No reuse allowed without permission.

Title: A Novel Temperature Controlled Bipolar Radiofrequency Ablation: An Ex Vivo Study for Optimizing Efficacy and Safety Parameters

Running title; A Temperature Controlled Bipolar Radiofrequency Ablation

Osamu Inaba M.D.[a], Yukihiro Inamura M.D.[a], Takamitsu Takagi M.D.[a], Shin Meguro M.D. [a], Kentaro Nakata M.D.[a], Toshiki Michishita M.D.[a], Yuhei Isonaga M.D.[a], Shinichi Tachibana M.D.[a], Hiroaki Ohya M.D.[a], Akira Sato M.D.[a], Shinsuke Miyazaki M.D.[b], Yasuteru Yamauchi M.D.[c], Masahiko Goya M.D.[d], Junichi Nitta M.D.[e], and Tetsuo Sasano M.D.[b]

a) Department of Cardiology, Japanese Red Cross Saitama Hospital, Saitama, Japan
b) Department of Cardiovascular Medicine, Institute of Science Tokyo, Tokyo, Japan
c) Department of Cardiology, Yokohama City Minato Red Cross Hospital, Yokohama, Japan.
d) Department of Cardiology, International University of Health and Welfare, Mita Hospital, Tokyo, Japan
e) Department of Cardiology, Sakakibara Heart Institute, Tokyo, Japan

Conflict of Interest: The authors have no conflicts to disclose about this article
Source of funding: none
Address for correspondence: Osamu Inaba, MD, Department of cardiology, Japanese Red Cross Saitama Hospital, Shin-Toshin 1-5, Chu-ou-ku, Saitama, 330-8553, Japan
81488521111
81488523120 (FAX)
e-mail oinbcvm@tmd.ac.jp
words count: 3537 words.

NOTE: This preprint reports new research that has not been certified by peer review and should not be used to guide clinical practice.

medRxiv preprint doi: https://doi.org/10.1101/2024.11.11.24317133; this version posted November 14, 2024. The copyright holder for this preprint (which was not certified by peer review) is the author/funder, who has granted medRxiv a license to display the preprint in perpetuity.
All rights reserved. No reuse allowed without permission.

Abstract

Background:

Bipolar radiofrequency catheter ablation (BRFA) is a potential treatment for refractory ventricular arrhythmias from deep myocardial tissue. However, clear indicators of efficacy and safety remain undefined.

Methods:

In an ex vivo model, BRFA was performed using either the QDOT Micro™ (QDT) or Thermocool SmartTouch SF™ as the active catheter, with the DiamondTemp Ablation™ (DTA) as the return catheter. Predictors of transmural lesion formation and steam-pop occurrence were assessed.

Results:

A total of 391 BRFA applications were performed with variations in the interelectrode distance between the active and return catheter tips, ranging from 6 to 27 mm, under various catheter tip and tissue contact configurations. The ablation index (AI) adjusted for inter-electrode distance effectively predicted transmural lesion formation. Logistic regression analysis revealed a coefficient for AI of -0.040 (SE: 0.0067; 95% CI: [-0.053, -0.027]; $p < 0.0001$) and for inter-electrode distance of 2.2 (SE: 0.35; 95% CI: [1.5, 2.9]; $p < 0.0001$). The decision boundary for transmural lesion formation was AI = 54 × inter-electrode distance – 260. When AI exceeded this value, sensitivity, specificity, and positive and negative predictive values for predicting transmural lesions were 89%, 92%, 91%, and 90%, respectively. When the AI was further increased by 50, the specificity reached 100%.

medRxiv preprint doi: https://doi.org/10.1101/2024.11.11.24317133; this version posted November 14, 2024. The copyright holder for this preprint (which was not certified by peer review) is the author/funder, who has granted medRxiv a license to display the preprint in perpetuity.
All rights reserved. No reuse allowed without permission.

Steam-pops on the active catheter side occurred only during power-controlled BRFA and were absent in temperature-controlled BRFA with a 45°C cutoff. On the return side, steam-pops occurred when DTA temperature exceeded 55°C, with deeper cracks observed above 60°C.

Conclusions:

An AI adjusted for inter-electrode distance strongly predicted transmural lesions. Temperature-controlled BRFA with a 45°C cutoff for QDT as the active catheter and 55°C for DTA as the return catheter may prevent steam-pops. Additionally, steam-pops occurring at higher catheter tip temperatures were associated with deeper tissue cracks.

medRxiv preprint doi: https://doi.org/10.1101/2024.11.11.24317133; this version posted November 14, 2024. The copyright holder for this preprint (which was not certified by peer review) is the author/funder, who has granted medRxiv a license to display the preprint in perpetuity.
All rights reserved. No reuse allowed without permission.

Clinical Perspective

What is known?

- Bipolar radiofrequency ablation has shown promise as an effective treatment option for ventricular arrhythmias originating from deep regions of the ventricular myocardium.
- The indicators for successful transmural lesion formation and the predictors for steam-pop are not yet well understood, and the accuracy of conventional metrics remains limited.

What the study adds

- The ablation index (AI) necessary for achieving successful transmural lesion formation during bipolar radiofrequency ablation, using a QDOT micro™ (QDT) as the active catheter and a DiamondTemp Ablation™ (DTA) the return catheter, can be determined using the formula: AI = 54 × inter-electrode distance – 260, where the inter-electrode distance denotes the distance between the active and return electrodes.
- During bipolar radiofrequency ablation, performing temperature-controlled ablation with a temperature cutoff of 45°C for the QDT and 55°C for the DTA may help prevent steam-pop.
- Furthermore, the higher the DTA temperature at the time of steam-pop, the deeper the cracks that are formed.

medRxiv preprint doi: https://doi.org/10.1101/2024.11.11.24317133; this version posted November 14, 2024. The copyright holder for this preprint (which was not certified by peer review) is the author/funder, who has granted medRxiv a license to display the preprint in perpetuity.
All rights reserved. No reuse allowed without permission.

Introduction

Radiofrequency (RF) catheter ablation is currently considered an effective option for the treatment of ventricular arrhythmias (VAs). Conventional unipolar radiofrequency ablation, which can be performed in conjunction with a variety of catheters and 3D mapping systems, is the standard method. However, its efficacy is limited when the origin of the VAs is intramural.

Bipolar RF catheter ablation (BRFA) is one of the next options for applying radiofrequency current to areas where it is difficult to form lesions deep enough using conventional unipolar ablation. (1) In BRFA, a RF current is passed between two catheters, an active catheter connected to the active port of the RF generator, and a return catheter connected to the indifferent electrode port instead of a return electrode patch, making it possible to form a deep ablation lesion between the two electrodes. The efficacy and safety of BRFA is gradually being recognized (2-5), but the cables connecting the generator and the return electrode are not widely commercially available and often have to be custom made. Furthermore, there are currently no established ablation settings or safety indicators for BRFA, and, because this is off-label use, catheter manufacturers also do not have sufficient data. Because serious complications of BRFA have been reported, it is important to establish efficacy and safety parameters of BRFA (6,7).

For conventional unipolar RF ablation, the ablation index (AI) was developed as a quantitative ablation lesion predictor, that includes contact force (CF), RF application time, and RF power in a weighted formula. The first aim of this study

medRxiv preprint doi: https://doi.org/10.1101/2024.11.11.24317133; this version posted November 14, 2024. The copyright holder for this preprint (which was not certified by peer review) is the author/funder, who has granted medRxiv a license to display the preprint in perpetuity.
All rights reserved. No reuse allowed without permission.

examined whether AI could be used to predict intermural lesion formation in BRFA as an efficacy parameter.

For a safety indicator, we focused on monitoring electrode temperature during BRFA. Recently, we reported a case of ventricular tachycardia in which temperature-controlled BRFA was successfully performed from both the endocardium and epicardium using a diamond embedded tip catheter (DiamondTemp Ablation [DTA] system [Medtronic, Inc., Minneapolis, Minnesota, USA]). (8) In temperature-controlled mode, the RF output is attenuated as the tissue surface temperature increases, potentially preventing steam-pop. DTA is open-irrigated but can measure the temperature of the tissue surface with high sensitivity, making temperature-controlled ablation possible.

Furthermore, in recent years, QDOT micro™ (QDT); Biosense Webstar, Irvine, California, USA have become widely available, enabling temperature-controlled ablation using the CARTO (Biosense Webstar, Irvine, California, USA). In the latter aim of the study, the safety of temperature-controlled BRFA and the relationship between electrode temperature and steam-pop during BRFA were investigated.

Methods

Fresh porcine ventricles were obtained commercially within 48 hours of sacrifice. A porcine ventricular tissue was fixed in a water pool filled with 37-degree saline, and an active catheter was perpendicularly placed on the endocardial side and a return catheter on the epicardial side. In this ex vivo study, we used a Thermocool SMARTTOUCH SF™ (STSF); Biosense Webstar, Irvine, California, USA or a QDT, which is capable of

medRxiv preprint doi: https://doi.org/10.1101/2024.11.11.24317133; this version posted November 14, 2024. The copyright holder for this preprint (which was not certified by peer review) is the author/funder, who has granted medRxiv a license to display the preprint in perpetuity.
All rights reserved. No reuse allowed without permission.

monitoring AI during RF application as the active catheter and a DTA as the return catheter to examine the usefulness of the ablation index in BRFA using the CARTO system.

An active catheter was connected to the active port of the radiofrequency generator of CARTO (nGEN, Biosense Webstar, Irvine, California, USA), and DTA as a return catheter was connected to ground electrode port of nGEN via generator connection box and pin box using alligator clip. (Figure 1 Main)

This study was divided into two parts. In the first part, to investigate the optimal AI value for forming an intermural lesion, QDT and DTA were attached to ventricular muscle tissue in four configurations: both perpendicular with slight angle, QDT perpendicular and DTA parallel, both parallel, and QDT parallel and DTA perpendicular (Model 1A, B, C, D, Figure 1 A, B, C, D). In this process, since previous studies have reported that proper attachment of the second ring electrode in DTA is crucial, it was slightly angled to ensure the second electrode contacted with the tissue before applying the BRFA when attaching DTA perpendicularly. (9)

The purpose of the second part was to examine steam-pop prediction. Both QDT and STSF were used as active catheters, and to make audible steam-pop more likely to occur, the DTA electrode was inserted between the myocardium and a synthetic resin base and attached parallel to the myocardium to concentrate the RF current in a narrower area and make it easier to raise the tissue temperature. (Model 2, Figure 1E).

In addition to these ablation sets, another lesion set was examined where only the distal thin-tip electrode of the DTA was completely perpendicularly attached to the tissue for current application. (Model 3, Figure 1F)

medRxiv preprint doi: https://doi.org/10.1101/2024.11.11.24317133; this version posted November 14, 2024. The copyright holder for this preprint (which was not certified by peer review) is the author/funder, who has granted medRxiv a license to display the preprint in perpetuity.
All rights reserved. No reuse allowed without permission.

In each model, the target AI was set, and ablation was started with a CF of about 5 to 15 g and a power output of 25 to 40 W. For all ablations using QDT, QMODE^{TM} was used with a temperature cutoff set at 45 °C. The irrigation flow for BRFA using the QDT was regulated by temperature control with QMODE^{TM}, while for BRFA using the STSF, it was set to 15 ml/min higher than 30W, and 8 ml/min at 30W or lower. The irrigation flow for the DTA was manually set to 8 ml/min during RF delivery. Ablation was stopped when an audible steam-pop occurred. The temperature and impedance of the DTA were visually monitored and recorded.

After ablation, myocardial sections were cut and visually inspected to confirm whether transmural lesions were formed. Additionally, the distance between the two electrodes where BRFA was performed was measured. The target AI was gradually increased from a lower initial value until transmural lesions were formed. For sections where a steam-pop occurred, the specific side of the catheter where the steam-pop occurred was visually recorded in addition to noting the tactile sensation experienced by the catheter operator. Furthermore, the extent of the cracks was also measured. During lesion confirmation, the measurers were blinded to the AI and the type of active catheter used.

In the examination of the effectiveness of AI, for both Model 1 and Model 2, the AI, the distance between electrodes of QDT/STSF and DTA used in BRFA (inter-electrode distance), CF, BRFA duration, energy, circuit impedance drop rate (% Impedance drop), temperature of the DTA and the values of AI, BRFA duration, and energy divided by the inter-electrode distance (AI/inter-electrode distance, BRFA

medRxiv preprint doi: https://doi.org/10.1101/2024.11.11.24317133; this version posted November 14, 2024. The copyright holder for this preprint (which was not certified by peer review) is the author/funder, who has granted medRxiv a license to display the preprint in perpetuity.
All rights reserved. No reuse allowed without permission.

duration/inter-electrode distance and energy/inter-electrode distance) were investigated for ablations that resulted in transmural lesions and those that did not.

In the examination of steam-pops, the same parameters were investigated for sections where steam-pops occurred and those where they did not. Additionally, the depth of the cracks caused by steam-pop was classified into four categories: less than 25% of the surface or not visible to the naked eye, 25% to 50% of the surface, more than 50% of the surface with partial incompleteness, and through-wall cracks. This study was performed in accordance with the Guide for the Care and Use of Laboratory Animals published by the U.S. National Institutes of Health.

Statistical Analysis

Continuous data are given as mean ± standard deviation if normally distributed or the median, maximum, and minimum values if not normally distributed. Categorical data are given as counts and percentages. Continuous data were compared using Student's t test or one-way analysis of variance when normally distributed or Mann-Whitney U test when not normally distributed. Categorical data were compared using χ^2 test across the groups.

Factors related to the formation of transmural lesions were analyzed using univariate analysis, and the relationship between those factors and inter-electrode distance was examined on a scatter plot. Furthermore, on that scatter plot, the BRFA application groups that could and could not form transmural lesions were depicted separately. A logistic regression model was employed to determine the decision boundary between the groups. The decision boundary, where the probability of an observed value belonging to the transmural lesion group is 0.5, was plotted, and the

medRxiv preprint doi: https://doi.org/10.1101/2024.11.11.24317133; this version posted November 14, 2024. The copyright holder for this preprint (which was not certified by peer review) is the author/funder, who has granted medRxiv a license to display the preprint in perpetuity.
All rights reserved. No reuse allowed without permission.

equations related to the formation of transmural lesions based on the inter-electrode distance required for lesion formation were derived. Additionally, the sensitivity, specificity, and positive and negative predictive values of BRFA applications beyond the AI threshold—calculated based on electrode distance using the decision boundary formula—were assessed for their effectiveness in predicting transmural lesion formation. The level of significance was set at $P<0.05$.

Analyses were performed with JMP® 14 (SAS Institute Inc., Cary, NC).

Results

Evaluation of AI and Transmural Lesion Formation

In total, 391 BRFA were performed on slices of varying thickness with inter-electrode distances ranging from 6 to 27 mm, and no damage occurred to the CARTO system or the generators of CARTO and DTA. Two-hundred-thirty-three ablations were performed in Model 1 and 148 ablations in Model 2, resulting in 127 transmural lesions in Model 1 and 109 transmural lesions in Model 2.

In Model 1 overall, except for the average CF, average power and maximum temperature of DTA, all parameters showed higher values in the ablations where transmural lesions were formed (AI: 680±240, 580±200, p=0.0005; AI/inter-electrode distance: 46±7.6, 32±5.8, $p<0.0001$; BRFA duration: 64 [6.2 - 630], 40 [3.7 - 520], p=0.0004; BRFA duration/inter-electrode distance: 4.7 [0.62 - 23], 2.2 [0.32 - 21], $p<0.0001$; Energy: 2300 [220 - 220000], 1500 [130 - 14000], p=0.0011; Energy/inter-electrode distance: 150 [11 - 820], 100 [12 - 560], $p<0.0001$; maximum % Impedance drop: 16±4.1, 13±3.4, $p<0.0001$; inter-electrode distance : 14 [6 - 27], 18

medRxiv preprint doi: https://doi.org/10.1101/2024.11.11.24317133; this version posted November 14, 2024. The copyright holder for this preprint (which was not certified by peer review) is the author/funder, who has granted medRxiv a license to display the preprint in perpetuity.
All rights reserved. No reuse allowed without permission.

[8 - 27], p<0.0001) (Table 1). Among these, only AI/interelectrode distance and BRFA duration/inter-electrode distance showed significantly higher values in the ablations where transmural lesions were formed across all variations of catheter tip configurations from Model 1A to 1D. (Supplemental Table 1)

As the inter-electrode distance increases, the AI required for transmural lesion formation increases linearly. (Figure 2A) Logistic regression analysis revealed that the regression coefficient for AI was -0.040 (standard error: 0.0067; 95% confidence interval: [-0.053, -0.027]; $p < 0.0001$), while the regression coefficient for inter-electrode distance was 2.2 (standard error: 0.35; 95% confidence interval: [1.5, 2.9]; $p < 0.0001$). Based on these results, the decision boundary for achieving or not achieving transmural lesion was calculated as: AI = 54 × inter-electrode distance − 260. Out of the 127 ablations where transmural lesions were formed, 117 ablations had AI values exceeding the decision boundary formula, while out of the 106 ablations where transmural lesions were not formed, 94 ablations had AI values below the decision boundary formula. The sensitivity, specificity, and positive and negative predictive values of the decision boundary for transmural lesion formation were 89%, 92%, 91%, and 90%, respectively. The relationship between AI and inter-electrode distance for ablations that achieved transmural lesion formation and those that did not, in each catheter tip configuration, is shown in the Supplemental Figure 1.

Regarding the analysis of BRFA duration, it was observed from the scatter plot that taking the natural logarithm of BRFA duration (ln (BRFA duration)) reveals a linear boundary between ablations that formed transmural lesions and those that did not. In logistic regression analysis, the regression coefficient for the natural logarithm of BRFA

medRxiv preprint doi: https://doi.org/10.1101/2024.11.11.24317133; this version posted November 14, 2024. The copyright holder for this preprint (which was not certified by peer review) is the author/funder, who has granted medRxiv a license to display the preprint in perpetuity.
All rights reserved. No reuse allowed without permission.

duration was -7.0 (standard error: 1.1; 95% confidence interval [-9.3, -5.1], $p < 0.0001$), and the regression coefficient for the inter-electrode distance was 1.6 (standard error: 0.25; 95% confidence interval [1.2, 2.2], $p < 0.0001$). The decision boundary for achieving or not achieving transmural lesion was calculated as: ln (BRFA duration) = 0.23 × inter-electrode distance + 0.16. (Figure 2B) Similarly to the AI analysis, the sensitivity, specificity, and positive and negative predictive values for the decision boundary for transmural lesion formation based on ln (BRFA duration) were calculated as 95%, 85%, 88%, and 94%, respectively.

Evaluation of Steam-Pop

In Model 2, A total of 123 temperature-controlled ablations using QDT and 25 power-controlled ablations using STSF were performed, and 46 steam-pops were observed. Meanwhile, in Model 1, where all ablations were performed with temperature control, only 3 steam-pops occurred out of 233 applications.

All the steam-pops in Model 1 occurred on the return catheter side 47 to 67 seconds after the start of the ablation. At that time, the % Impedance drop was 17 to 21%, the temperature of DTA was 58 to 71 degrees, and the crack penetration depth was less than 50%. In Model 2, a comparison between 102 ablations without steam-pop and 46 ablations with steam-pop revealed that temperature-controlled ablations were more frequent in the ablations without steam-pop, whereas power-controlled ablations were more common in the ablation with steam-pop. In temperature-controlled ablations, all 32 steam-pops occurred on the return electrode side, while in power-controlled ablations, one steam-pop occurred on the active electrode side and the last 13 steam-pops occurred on the return electrode side. The ablations with steam-pops had significantly higher for

medRxiv preprint doi: https://doi.org/10.1101/2024.11.11.24317133; this version posted November 14, 2024. The copyright holder for this preprint (which was not certified by peer review) is the author/funder, who has granted medRxiv a license to display the preprint in perpetuity.
All rights reserved. No reuse allowed without permission.

average power, % Impedance drop, and DTA temperature compared to the ablations without steam-pops (Average Power: 28±10, 35±5.9, p<0.0001; maximum % Impedance drop: 22±6.2, 25±3.7, p=0.0007; maximum temperature of DTA: 60±7.7, 66±5.3, p<0.0001) (Table 2).

Among the 46 steam-pops that occurred in Model 2, an analysis of the 45 instances that occurred on the DTA side revealed that all steam-pops occurred when the DTA temperature 55 °C or higher, and the % Impedance drop exceeded 13Ω. Steam-pop did not occur when the DTA temperature was below 55°C or when the % Impedance drop was less than 13Ω. Figure 3A shows a plot of the maximum temperature of the DTA during ablation where steam-pop did not occur and the DTA temperature at the time of steam-pop during ablation where steam-pop occurred. When the DTA temperature cutoff is set at 55°C, the sensitivity, specificity, positive predictive value, and negative predictive value for predicting steam-pop occurrence are 100%, 27%, 38%, and 100%, respectively.

Similarly, Figure 3B shows a plot of the % Impedance drop. When the %Imp drop cutoff is set at 13%, the sensitivity, specificity, positive predictive value, and negative predictive value for predicting steam-pop occurrence are 100%, 8.8%, 33%, and 100%, respectively.

Furthermore, the higher the DTA temperature when steam-pop occurred, the larger the cracks that formed. The cracks penetrating 25% or more of the depth were observed only when the DTA temperature was 60 °C or higher. Cracks confined to the mid-myocardium were not observed in these ablations. (Figure 4A) A similar result was

medRxiv preprint doi: https://doi.org/10.1101/2024.11.11.24317133; this version posted November 14, 2024. The copyright holder for this preprint (which was not certified by peer review) is the author/funder, who has granted medRxiv a license to display the preprint in perpetuity.
All rights reserved. No reuse allowed without permission.

also observed with the % Impedance drop at steam-pop. Cracks that extended beyond 50% were only formed when the % Impedance drop exceeded 21%. (Figure 4B)

Model 3: A special catheter configuration

Lastly, 10 BRFA procedures were performed in Model 3, where only the distal 0.6 mm electrode of the DTA was attached to the myocardial tissue, and the second electrode was not attached. BRFA procedures with AI 400-750 were applied to myocardial tissue with an inter-electrode distance of 11 mm to 15 mm. However, no transmural lesions were formed, and lesion formation on the return electrode side was either absent or minimal. The highest temperature of the DTA remained below 46 °C. (Table 3)

Discussion

This study is the first ex vivo study to investigate transmurality and steam-pop occurrence in BRFA using QDT and DTA. This study has three notable points. First, it was found that performing BRFA using QDT as the active catheter and DTA as the return catheter is likely to not cause malfunctions with the system used in this study. As previously mentioned, BRFA is an off-label use, and the catheter manufacturers do not have data regarding potential system malfunctions. Therefore, the fact that nearly 400 BRFA procedures did not cause any issues with the CARTO system or the DTA generator is valuable information.

Second, this is the first report to confirm that AI can predict transmural lesion formation in BRFA. Previous studies have reported that factors related to transmurality in BRFA include total energy (10), thickness of the myocardium (11), use of a 3.5mm tip irrigated catheter (11), BRFA duration (12), impedance drop (12) and contact surface area of the return catheter (13). The results of the present study indicated that the

medRxiv preprint doi: https://doi.org/10.1101/2024.11.11.24317133; this version posted November 14, 2024. The copyright holder for this preprint (which was not certified by peer review) is the author/funder, who has granted medRxiv a license to display the preprint in perpetuity.
All rights reserved. No reuse allowed without permission.

313 inter-electrode distance and the corresponding AI or BRFA duration were crucial in
314 transmural lesion formation. As the inter-electrode distance increased, the AI and the ln
315 (BRFA duration) required to achieve transmural lesion formation increased linearly up
316 to an inter-electrode distance of 27 mm. In this study, both AI and ln (BRFA duration)
317 yielded highly accurate predictive formulas for achieving transmural lesion formation.
318 This may be attributed to the fact that the CF of the active catheter was controlled
319 around 10 g and the power was controlled at approximately 35W.

320 When performing BRFA under this study setting, it is considered more
321 reasonable to use AI for the following reasons. First, if BRFA were conducted with a
322 wider range of CF and power, the results might differ. Second, AI is automatically
323 calculated and does not require logarithmic computation. Third, the predictive formula
324 for transmural lesion formation using AI has higher specificity compared to the one
325 using ln (BRFA duration). To further increase the specificity of transmural lesion
326 formation, adding 50 to the calculated AI value from this equation could achieve 100%
327 specificity for transmural lesion formation.

328 The third notable point of this study is the potential for electrode temperature
329 monitoring to predict steam-pop occurrence. The factors related with steam-pop
330 occurrence during BRFA were previously reported as impedance drop (9) (14),
331 temperature of endocardial catheter (10), RF time (12) and high power (12) but
332 regarding impedance drop, there are also conflicting reports (15). In unipolar ablation,
333 Leshem et al. reported that temperature-controlled ablation using QDOT can create
334 comparable lesion formation without increasing the incidence of steam-pop compared to
335 power-controlled ablation (16). In their study, no steam-pop occurred when the targeted

medRxiv preprint doi: https://doi.org/10.1101/2024.11.11.24317133; this version posted November 14, 2024. The copyright holder for this preprint (which was not certified by peer review) is the author/funder, who has granted medRxiv a license to display the preprint in perpetuity.
All rights reserved. No reuse allowed without permission.

temperature of QDOT was set to 45°C, while steam-pop did occur when set to 50°C, though it was less frequent compared to power-controlled ablation. Nomura et al. reported that regarding DTA, steam-pop occurred only when the catheter tip of the DTA was applied perpendicularly during ablation with a targeted temperature set at 58°C (17). Al-Sheikhli et al. reported that steam-pop and cardiac tamponade occurred in one patient during one of 10 VT ablations with DTA, using a default target temperature of 60°C and an initial power of 50 W (18).

The results of the study showed that temperature-controlled BRFA using QMODE with a cutoff of 45°C could prevent steam-pops on the active catheter side. Additionally, no steam-pops occurred when the temperature of the opposing DTA remained below 55°C. In BRFA, the area most likely to be heated is directly beneath the contact points between the tissue and each of the two electrodes where the radiofrequency current converges, as suggested by computer simulation models. (19) Therefore, monitoring the surface temperature of both electrodes to prevent steam-pop at each location is valuable. From these results, it is suggested that during QMODE ablation set at 45°C, visually monitoring the temperature of the opposing DTA and manually reducing the output of QDT when the temperature exceeds 55°C may help prevent steam-pops on both sides. Using a non-irrigated tip catheter as the return catheter allows for the measurement of the myocardial surface temperature on the opposite side; however, if the tip is not irrigated, there is a risk of thrombosis. While an irrigated tip might cool the temperature sensor itself, DTA, utilizing the high thermal conductivity of diamond, enables effective temperature monitoring. Therefore, using DTA as the return catheter is reasonable. In this study, % Impedance drop was also

medRxiv preprint doi: https://doi.org/10.1101/2024.11.11.24317133; this version posted November 14, 2024. The copyright holder for this preprint (which was not certified by peer review) is the author/funder, who has granted medRxiv a license to display the preprint in perpetuity.
All rights reserved. No reuse allowed without permission.

useful for predicting steam-pop. Saito et al. reported that the frequency of steam-pop decreased when BRFA was performed with reduced power according to the %Imp drop. (20) In this study, it was not verified whether controlling the power output according to DTA temperature could prevent steam-pop. However, in terms of steam-pop occurrence, DTA temperature had much higher specificity compared to % Impedance drop. This result is likely because % Impedance drop can be influenced by the temperature increase in all regions through which the radiofrequency current flows, whereas DTA can measure the temperature specifically in the tissue surface where the catheter tip makes contact, which is near the region most susceptible to steam-pop occurrence.

In the validation of Model 3, lesions were hardly formed when only the distal small tip of the DTA was in contact with the tissue during ablation. This was likely because the proximal larger tip of the DTA was floating in the saline, causing the radiofrequency current to bypass the myocardial tissue and flow from the saline to the proximal larger tip, resulting in insufficient heating of the tissue. The distal small tip is 0.6 mm long, and in practice, it is unlikely that only this electrode would make contact with the tissue. However, if, as indicated by the results of this study, there is little temperature rise in the DTA, it may be worth considering adjusting the positioning of the DTA to ensure effective ablation.

Study Limitations

This study has some limitations. As mentioned earlier, CF and power were controlled to some extent in this study, and altering the range of these parameters could lead to

medRxiv preprint doi: https://doi.org/10.1101/2024.11.11.24317133; this version posted November 14, 2024. The copyright holder for this preprint (which was not certified by peer review) is the author/funder, who has granted medRxiv a license to display the preprint in perpetuity.
All rights reserved. No reuse allowed without permission.

different results. Second, it is unclear whether similar results would be obtained with BRFA using an inter-electrode distance of 28 mm or more.

Conclusions

AI adjusted for inter-electrode distance proved to be highly significant for achieving transmural lesion formation during BRFA. Furthermore, temperature-controlled ablation using QDT and DTA demonstrated potential for predicting steam-pop during BRFA.

References

1) Victor Neira, Pasquale Santangeli, Piotr Futyma, John Sapp, Miguel Valderrabano, Fermin Garcia, Andres Enriquez. Heart Rhythm. 2020 Jul;17:1176-1184.
2) Igarashi M, Nogami A, Fukamizu S, et al. Acute and long-term results of bipolar radiofrequency catheter ablation of refractory ventricular arrhythmias of deep intramural origin. Heart Rhythm. 2020;17:1500-7.
3) Futyma P, Ciąpała K, Głuszczyk R, et al. Bipolar ablation of refractory atrial and ventricular arrhythmias: Importance of temperature values of intracardiac return electrodes. J Cardiovasc Electrophysiol. 2019;30:1718-26.
4) Futyma P, Ciapala K, Sander J, et al. Bipolar Radiofrequency Ablation of Ventricular Arrhythmias Originating in the Vicinity of His Bundle. Circ Arrhythm Electrophysiol . 2020 Mar;13:e008165.
5) Andres Enriquez, Matthew Hanson, Babak Nazer, Douglas N Gibson, Oscar Cano, Sayuri Tokioka, Seiji Fukamizu, Pablo Sanchez Millan, Carolina Hoyos, Carlos Matos, William H Sauer, Usha Tedrow, Jorge Romero, Victor Neira, Marian Futyma, Piotr Futyma. Bipolar ablation involving coronary venous system for refractory left ventricular summit arrhythmias. Heart Rhythm O2. 2023 Nov 24; 5:24-33.

medRxiv preprint doi: https://doi.org/10.1101/2024.11.11.24317133; this version posted November 14, 2024. The copyright holder for this preprint (which was not certified by peer review) is the author/funder, who has granted medRxiv a license to display the preprint in perpetuity.
All rights reserved. No reuse allowed without permission.

6) Timothy R Maher, Adnan S Raza, Carlos Tapias, Fermin Garcia, Matthew R Reynolds, G Muqtada Chaudry, Luis C Saenz, Miguel Valderrábano, Andre d'Avila. Ventricular septal defect as a complication of bipolar radiofrequency ablation for ventricular tachycardia. Heart Rhythm. 2024 Jun;21: 950-955.

7) Piotr Kulakowski, Pawel Derejko, Jacek Kusnierz, Jakub Baran, Urszula Hangiel, Izabela Janus, Agnieszka Noszczyk-Nowak. Fatal Complication of Endo-Epicardial Bipolar Radiofrequency Ablation During Animal Experiment. JACC Clin Electrophysiol. 2023 Jun;9:886-888.

8) Osamu Inaba, Yukihiro Inamura, Takamitsu Takagi, Akira Sato, Masahiko Goya, Tetsuo Sasano. First Experience of Temperature-Controlled Bipolar Radiofrequency Ablation of Ventricular Tachycardia Originating from the Anterior Left Ventricle Using a Diamond Embedded Tip Catheter. HeartRhythm Case Rep. 2023 May 18;9:529-533.

9) Sho Ogiso, Hidehira Fukaya, Emiyu Ogawa, Hitoshi Mori, Yuya Masuda, Yuto Yazaki, Yusuke Murayama, Daiki Saito, Shuhei Kobayashi, Hironori Nakamura, Naruya Ishizue, Jun Kishihara, Shinichi Niwano, Jun Oikawa, Junya Ako. "Honey pot"-like lesion formation: Impact of catheter contact angle on lesion formation by novel diamond-embedded temperature-controlled ablation catheter in a porcine experimental model. Heart Rhythm. 2024 May 15:S1547-5271(24)02569-4.

10) Paweł Derejko, Izabela Janus, Piotr Kułakowski, Jacek Kuśnierz, Jakub Baran, Urszula Hangiel, Joanna Proszek, Piotr Frydrychowski, Marcin Michałek, Agnieszka Noszczyk-Nowak et al. Bipolar endo-epicardial RF ablation: Animal feasibility study Heart Rhythm. 2024 Jun;21(6):790-798.

medRxiv preprint doi: https://doi.org/10.1101/2024.11.11.24317133; this version posted November 14, 2024. The copyright holder for this preprint (which was not certified by peer review) is the author/funder, who has granted medRxiv a license to display the preprint in perpetuity.
All rights reserved. No reuse allowed without permission.

11) Duy T Nguyen, Wendy S Tzou, Michael Brunnquell, Matthew Zipse, Joseph L Schuller, Lijun Zheng, Ryan A Aleong, William H Sauer. Clinical and biophysical evaluation of variable bipolar configurations during radiofrequency ablation for treatment of ventricular arrhythmias. Heart Rhythm. 2016 Nov;13(11):2161-2171.

12) Mathews John, Ashley Rook, Allison Post, Alton Mersman, Whitney Allen, Christina Schramm, Mehdi Razavi. Bipolar ablation's unique paradigm: Duration and power as respectively distinct primary determinants of transmurality and steam pop formation. Heart Rhythm O2. 2020 Jun 24;1(4):290-296.

13) Arwa Younis, Hagai D Yavin, Koji Higuchi, Israel Zilberman, Jakub Sroubek, Patrick Tchou, Zachary P Bubar, Michael Barkagan, Eran Leshem, Ayelet Shapira-Daniels, Mohamad Kanj, Daniel J Cantillon, Ayman A Hussein, Khaldoun G Tarakji, Walid I Saliba, Jacob S Koruth, Elad Anter. Increasing Lesion Dimensions of Bipolar Ablation by Modulating the Surface Area of the Return Electrode. JACC Clin Electrophysiol. 2022 Apr;8(4):498-510.

14) Abhishek Bhaskaran, Ahmed Niri, Mohammed Ali Azam, Sachin Nayyar, Andreu Porta-Sánchez, Stéphane Massé, Timothy Liang, Arulalan Veluppillai, Beibei Du, Patrick F H Lai, Andrew Ha, Kumaraswamy Nanthakumar. Safety, efficacy, and monitoring of bipolar radiofrequency ablation in beating myopathic human and healthy swine hearts Heart Rhythm. 2021 Oct;18(10):1772-1779.

15) Shinwan Kany, Fares Alexander Alken, Ruben Schleberger, Jakub Baran, Armin Luik, Annika Haas, Elena Ene, Thomas Deneke, L Dinshaw, Andreas Rillig, Andreas Metzner, Bruno Reissmann, Hisaki Makimoto, Tilko Reents, Miruna Andrea Popa, Isabel Deisenhofer, Roman Piotrowski, Piotr Kulakowski, Paulus

medRxiv preprint doi: https://doi.org/10.1101/2024.11.11.24317133; this version posted November 14, 2024. The copyright holder for this preprint (which was not certified by peer review) is the author/funder, who has granted medRxiv a license to display the preprint in perpetuity.
All rights reserved. No reuse allowed without permission.

Kirchhof, Katharina Scherschel, Christian Meyer. Bipolar ablation of therapy-refractory ventricular arrhythmias: application of a dedicated approach. Europace. 2022 Jul 15;24(6):959-969.

16) Eran Leshem, Israel Zilberman, Michael Barkagan, Ayelet Shapira-Daniels, Jakub Sroubek, Assaf Govari, Alfred E Buxton, Elad Anter. Temperature-Controlled Radiofrequency Ablation Using Irrigated Catheters: Maximizing Ventricular Lesion Dimensions While Reducing Steam-Pop Formation. JACC Clin Electrophysiol 2020 Jan;6(1):83-93.

17) Takehiro Nomura, Manabu Maeda, Daiki Kumazawa, Yosuke Mizuno, Kosuke Onodera, Shigeru Toyoda, Kennosuke Yamashita. The effect of ablation settings on lesion characteristics with DiamondTemp ablation system: An ex vivo experiment. J Arrhythm. 2023 Dec 6;40(1):109-117.

18) Jaffar Al-Sheikhli, Ian Patchett, Ven Gee Lim, Leeann Marshall, Will Foster, Michael Kuehl, Shamil Yusuf, Sandeep Panikker, Kiran Patel, Faizel Osman, Prithwish Banerjee, Nicolas Lellouche, Tarvinder Dhanjal. Initial experience of temperature-controlled irrigated radiofrequency ablation for ischaemic cardiomyopathy ventricular tachycardia ablation. J Interv Card Electrophysiol. 2023 Apr;66(3):551-559.

19) Yao Sun, Xin Zhu, Wenxi Chen, Weihao Weng, Keijiro Nakamura. Computer simulation of low-power and long-duration bipolar radiofrequency ablation under various baseline impedances. Med Eng Phys . 2024 Sep:131:104226.

20) Osamu Saitoh, Takumi Kasai, Kyogo Fuse, Ayaka Oikawa, Hiroshi Furushima, Masaomi Chinushi. Impedance-decline-guide power control long application time

medRxiv preprint doi: https://doi.org/10.1101/2024.11.11.24317133; this version posted November 14, 2024. The copyright holder for this preprint (which was not certified by peer review) is the author/funder, who has granted medRxiv a license to display the preprint in perpetuity.
All rights reserved. No reuse allowed without permission.

473 bipolar radiofrequency catheter ablation. J Cardiovasc Electrophysiol. 2022
474 Dec;33(12):2538-2545.
475

medRxiv preprint doi: https://doi.org/10.1101/2024.11.11.24317133; this version posted November 14, 2024. The copyright holder for this preprint (which was not certified by peer review) is the author/funder, who has granted medRxiv a license to display the preprint in perpetuity.
All rights reserved. No reuse allowed without permission.

476 Table 1. Comparison of BRFA parameters between ablations with and without

477 transmural lesion formation.

All catheter configurations in Model 1	transmural lesion (+) N = 127	transmural lesion (-) N = 106	
AI	680±240	580±200	0.0005
AI / inter-electrode distance	46±7.6	32±5.8	<0.0001
BRFA duration (sec)	64 [6.2 - 630]	40 [3.7 - 520]	0.0004
BRFA duration / inter-electrode distance	4.7 [0.62 - 23]	2.2 [0.32 - 21]	<0.0001
average CF (g)	11±2.9	11±2.4	0.34
average Power (W)	35±2.8	36±4.3	0.006
Energy (J)	2300 [220 - 220000]	1500 [130 - 14000]	0.0011
Energy / inter-electrode distance	150 [11 - 820]	100 [12 - 560]	<0.0001
maximum % Impedance drop	16±4.1	13±3.4	<0.0001
maximum temperature of DTA (degree)	60±5.4	59±6.5	0.24
Inter-electrode distance (mm)	14 [6 - 27]	18 [8 - 27]	<0.0001

478 BRFA, bipolar radiofrequency catheter ablation; AI, ablation index; inter-electrode

479 distance, the distance between electrodes; RF, radiofrequency; CF, contact force; %

480 Impedance drop, the rate of generator impedance drop; DTA, DiamondTemp Ablation

481

medRxiv preprint doi: https://doi.org/10.1101/2024.11.11.24317133; this version posted November 14, 2024. The copyright holder for this preprint (which was not certified by peer review) is the author/funder, who has granted medRxiv a license to display the preprint in perpetuity.
All rights reserved. No reuse allowed without permission.

Table 2. Comparison of protocols and parameters between ablations with and without steam-pop occurrence in Model 2.

	Steam-pop (-)	Steam-pop (+)	p value
Model 2	N = 102	N = 46	
Ablation mode			0.0062
Temperature-controled (QDT)	91(74%)	32(26%)	
Power-controled (STSF)	11(44%)	14(56%)	
Titration	41(40%)	10(20%)	0.019
The side of steam-pop		Active, STSF 1	
		Active, QDT 0	
		Return 45	
Average CF (g)	12±4.7	11±4.7	0.34
Average Power (w)	28±10	35±5.9	<0.0001
AI	570±210	550±120	0.52
% Impedance drop (%)			
at 3sec	8.7±2.7	9.7±1.9	0.029
at 5sec	11±3.5	13±2.4	0.0063
at 10sec	14±4.6	17±3.4	<0.0001
maximum	22±6.2	25±3.7	0.0007
when pop		24±4.3	
Temperature of DTA (degree)			
at10 sec	55±7.5	60±4.6	<0.0001
Maximum	60±7.7	66±5.3	<0.0001
when pop		65[55 - 75]	
Inter-electrode distance (mm)	15±4.6	14±3.7	0.016

medRxiv preprint doi: https://doi.org/10.1101/2024.11.11.24317133; this version posted November 14, 2024. The copyright holder for this preprint (which was not certified by peer review) is the author/funder, who has granted medRxiv a license to display the preprint in perpetuity.
All rights reserved. No reuse allowed without permission.

485 QDT, QDOT micro™; STSF, Thermocool SMARTTOUCH SF™, For other

486 abbreviations, see Table 1.

medRxiv preprint doi: https://doi.org/10.1101/2024.11.11.24317133; this version posted November 14, 2024. The copyright holder for this preprint (which was not certified by peer review) is the author/funder, who has granted medRxiv a license to display the preprint in perpetuity.
All rights reserved. No reuse allowed without permission.

487 Table 3. Ablation parameters and lesion depth and size on each electrode side during

488 BRFA performed with only the distal small tip of the DTA in contact with the tissue

Model 3	N = 10
AI	520±120
AI / inter-electrode distance	36±8.2
BRFA duration (sec)	32 [19 - 72]
RF time / inter-electrode distance	2.5 [1.3 - 5.1]
average CF (g)	11±4.1
average Power (W)	35
Energy (J)	1100 [670 - 2500]
Energy / inter-electrode distance	87 [45 - 180]
maximum % Impedance drop (%)	8.6±1.6
maximum temerature of DTA (degree)	45±0.67
Inter-electrode distance (mm)	15 [11 - 15]
Active electrode	
lesion depth (mm)	3.9±1.0
lesion short axis (mm)	5.8±1.1
Return electrode	
lesion depth (mm)	0 [0 - 2]
lesion short axis (mm)	0 [0 - 2]

489

490 Abbreviations are the same as in Table 1 and 2.

491

medRxiv preprint doi: https://doi.org/10.1101/2024.11.11.24317133; this version posted November 14, 2024. The copyright holder for this preprint (which was not certified by peer review) is the author/funder, who has granted medRxiv a license to display the preprint in perpetuity.
All rights reserved. No reuse allowed without permission.

492 Figure 1

Figure 1 Main

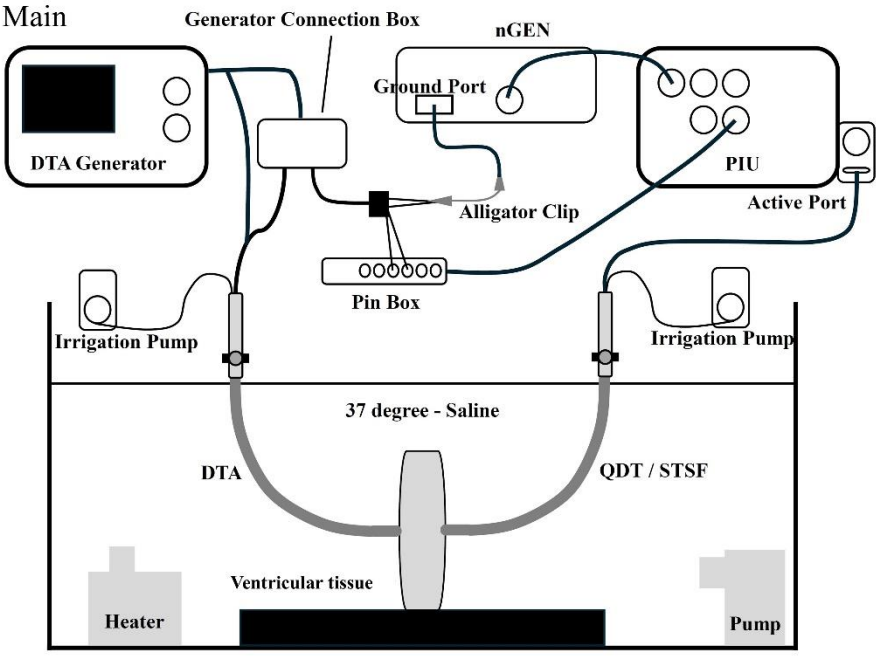

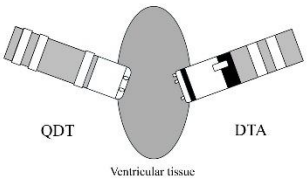

Figure 1A

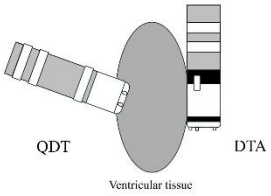

Figure 1B

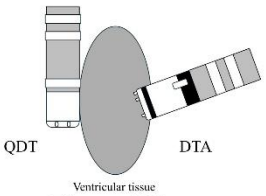

Figure 1C

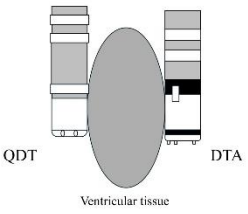

Figure 1D

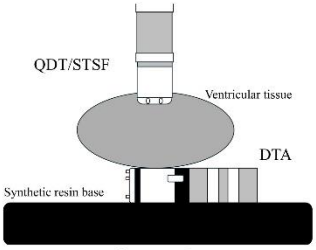

Figure 1E

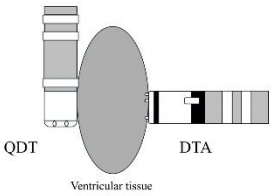

Figure 1F

493

medRxiv preprint doi: https://doi.org/10.1101/2024.11.11.24317133; this version posted November 14, 2024. The copyright holder for this preprint (which was not certified by peer review) is the author/funder, who has granted medRxiv a license to display the preprint in perpetuity.
All rights reserved. No reuse allowed without permission.

494 The circuit model for BRFA using CARTO and DTA is shown. The QDOT/STSF is
495 connected as the active catheter, attached to the active port in the usual manner. The
496 DTA is connected to the ground port via an alligator clip. To display the DTA on the
497 CARTO system during the experiment, only the proximal electrodes of the DTA are
498 connected to the patient interface unit of the CARTO system via the Pin box.
499 Furthermore, the contact patterns between each catheter tip and the ventricular
500 myocardium are shown in Figures 1A through 1F. Figures 1A to 1D illustrate four
501 different configurations where the QDOT and DTA were adhered perpendicularly
502 and parallel (Models 1A - 1D). Figure 1E shows a scenario in which the DTA was
503 sandwiched between the ventricular myocardium and a synthetic resin base to create
504 conditions prone to steam-pop formation (Model 2). Figure 1F shows a special
505 configuration in which only the 0.6 mm long distal small tip of the DTA is in contact
506 with the ventricular myocardium, while the proximal large tip is not in contact with
507 the tissue (Model 3). DTA, DiamondTemp Ablation™; nGEN, nGEN™ generator;
508 PIU, patient interface unit; QDT. QDOT micro™; STSF, Thermocool
509 SMARTTOUCH SF™;
510

medRxiv preprint doi: https://doi.org/10.1101/2024.11.11.24317133; this version posted November 14, 2024. The copyright holder for this preprint (which was not certified by peer review) is the author/funder, who has granted medRxiv a license to display the preprint in perpetuity.
All rights reserved. No reuse allowed without permission.

511 Figure 2

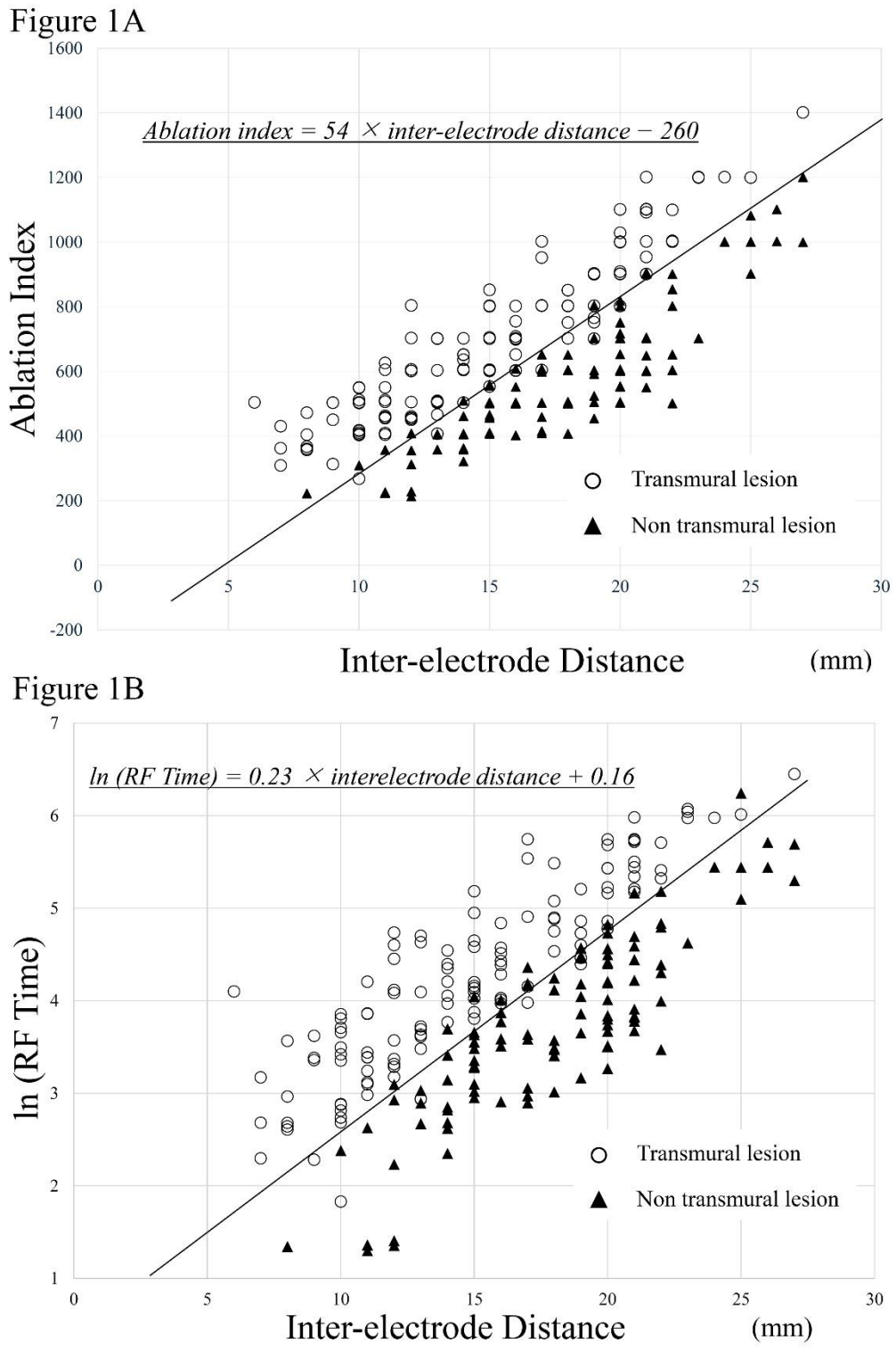

512

medRxiv preprint doi: https://doi.org/10.1101/2024.11.11.24317133; this version posted November 14, 2024. The copyright holder for this preprint (which was not certified by peer review) is the author/funder, who has granted medRxiv a license to display the preprint in perpetuity.
All rights reserved. No reuse allowed without permission.

513 The relationship between inter-electrode distance, AI, and the logarithm of BRFA
514 duration is displayed, separated into ablations with and without transmural lesion
515 formation. The AI and ln (BRFA duration) required to achieve transmural lesion
516 formation increase linearly as the inter-electrode distance increases. The decision
517 boundary equations for achieving and not achieving transmural lesion formation are
518 AI = 54 × inter-electrode distance − 260 and ln (BRFA duration) = 0.23 ×
519 interelectrode distance + 0.16, respectively. AI, ablation index; BRFA, bipolar
520 radiofrequency catheter ablation; inter-electrode distance, the distance between
521 electrodes used in BRFA
522

medRxiv preprint doi: https://doi.org/10.1101/2024.11.11.24317133; this version posted November 14, 2024. The copyright holder for this preprint (which was not certified by peer review) is the author/funder, who has granted medRxiv a license to display the preprint in perpetuity.
All rights reserved. No reuse allowed without permission.

523 Figure 3

Figure 3A

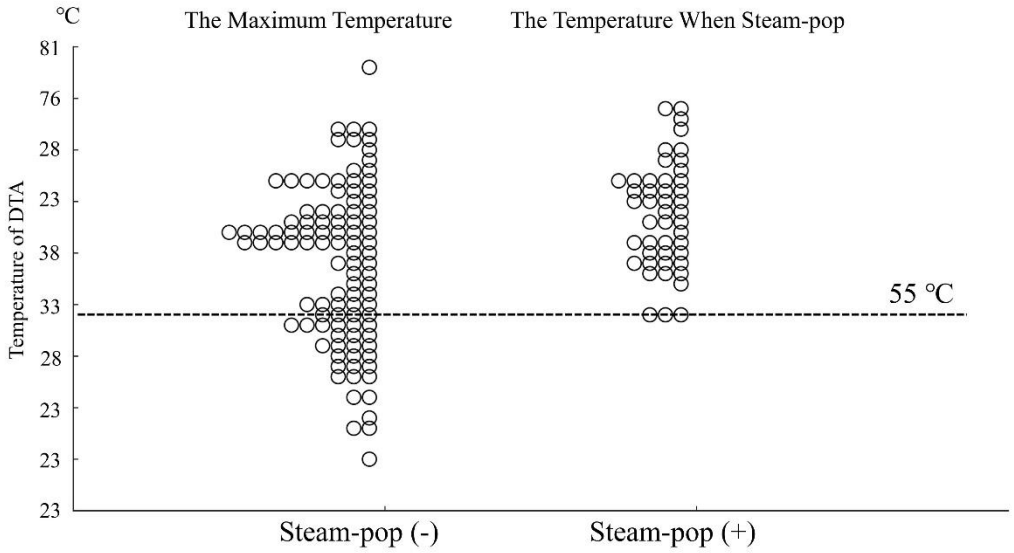

Figure 3B

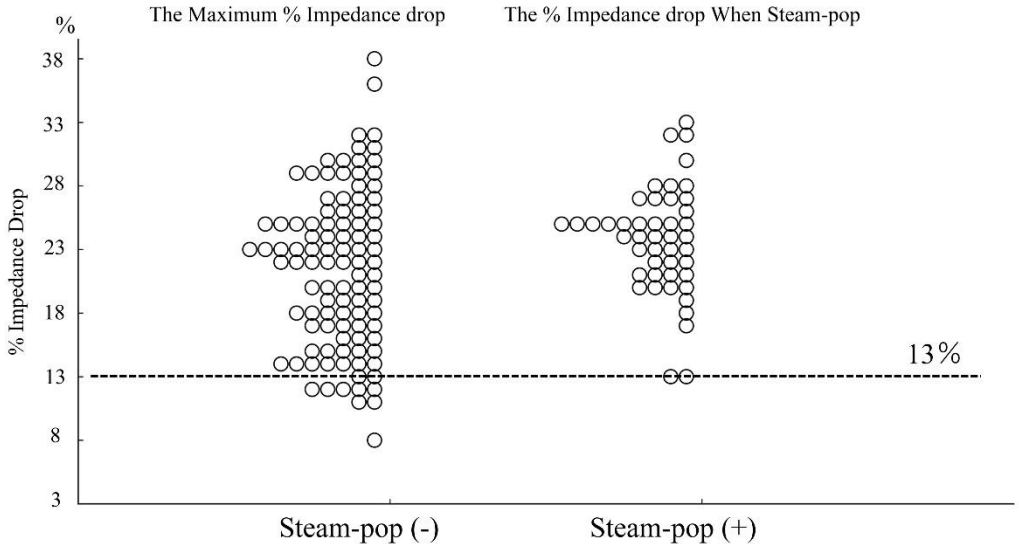

524

medRxiv preprint doi: https://doi.org/10.1101/2024.11.11.24317133; this version posted November 14, 2024. The copyright holder for this preprint (which was not certified by peer review) is the author/funder, who has granted medRxiv a license to display the preprint in perpetuity.
All rights reserved. No reuse allowed without permission.

525 Comparison of the maximum DTA temperature and maximum % Impedance drop in
526 ablation without steam-pop, and the DTA temperature and % Impedance drop at the
527 time of steam-pop in ablation where steam-pop occurred. Figure 3A shows that all
528 steam-pops occurred only when the DTA temperature was 55°C or higher. Similarly,
529 Figure 3B shows that all steam-pops occurred only when the % Impedance drop was
530 13% or higher.
531 DTA, DiamondTemp Ablation™; %Impedance drop, the rate of generator
532 impedance drop.
533

medRxiv preprint doi: https://doi.org/10.1101/2024.11.11.24317133; this version posted November 14, 2024. The copyright holder for this preprint (which was not certified by peer review) is the author/funder, who has granted medRxiv a license to display the preprint in perpetuity.
All rights reserved. No reuse allowed without permission.

534 Figure 4

Figure 4A

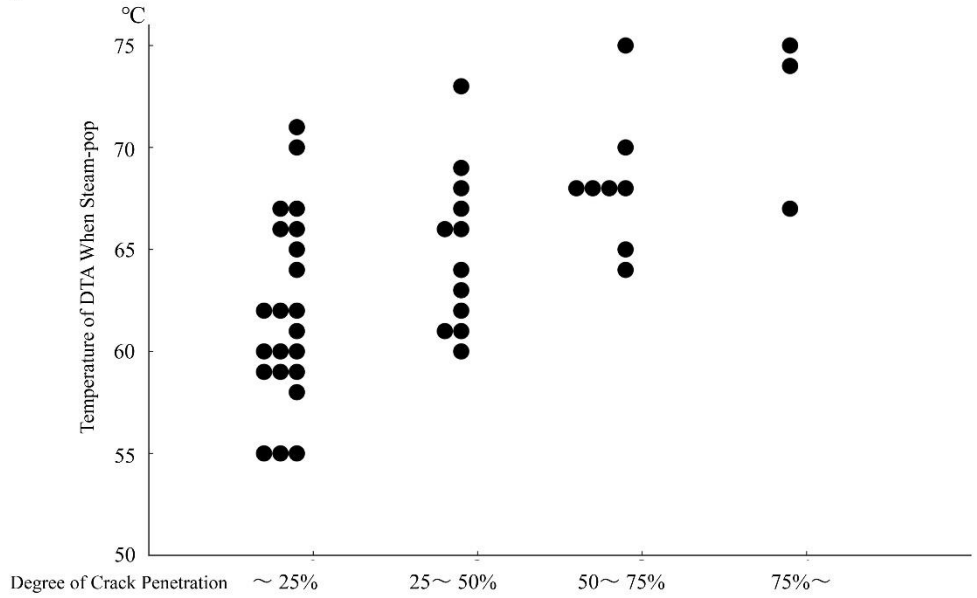

Figure 4B

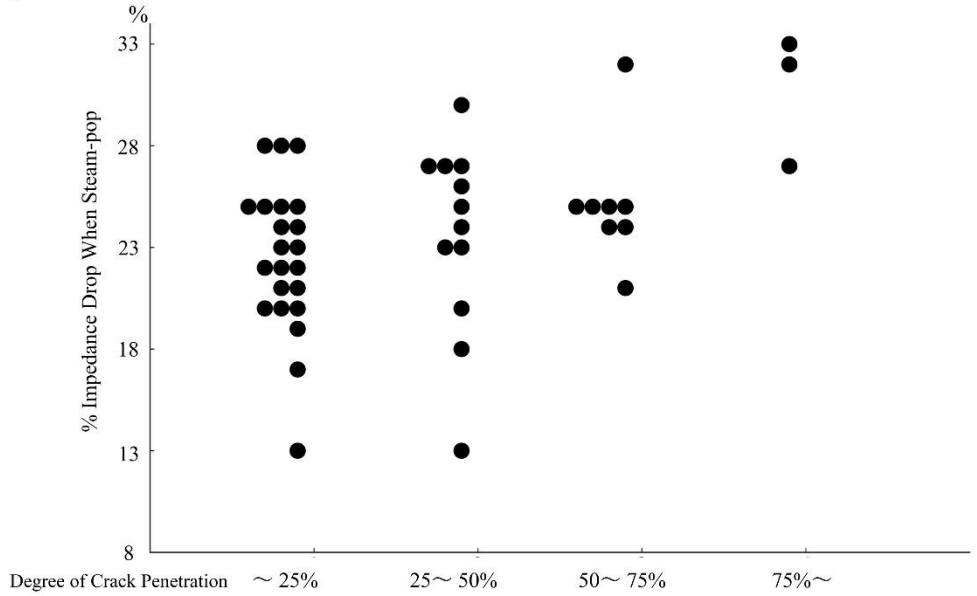

535

medRxiv preprint doi: https://doi.org/10.1101/2024.11.11.24317133; this version posted November 14, 2024. The copyright holder for this preprint (which was not certified by peer review) is the author/funder, who has granted medRxiv a license to display the preprint in perpetuity.
All rights reserved. No reuse allowed without permission.

536 The relationship between the depth of visually confirmed cracks in ablation where
537 steam-pop occurred, and the DTA temperature and % impedance drop at the time of
538 steam-pop. Cracks with a depth of 25% or more were observed only when
539 steam-pop occurred with the DTA temperature reaching 60°C or higher. (Figure 4A)
540 Similarly, cracks with a depth of 50% or more were observed only when the %
541 impedance drop increased by 21% or more. (Figure 4B)
542 Abbreviations are the same as in Figure 3.
543
544

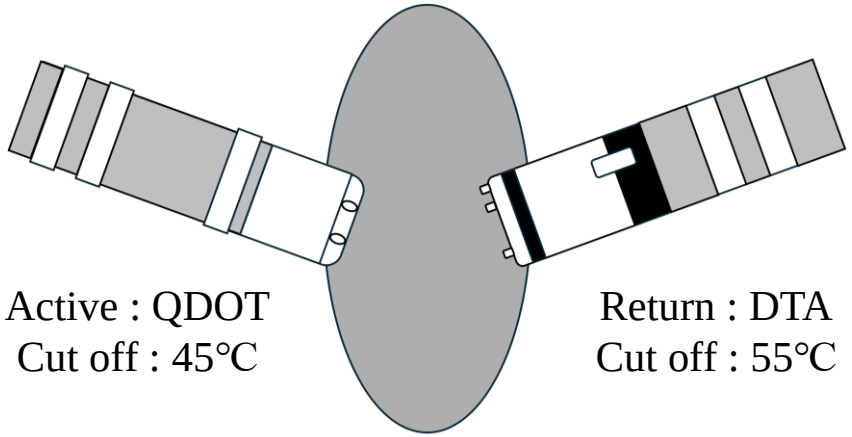

- ✓ When AI exceeds 54 × inter-electrode distance - 260, transmural lesion formation can be achieved with high accuracy.
- ✓ With a 45℃ cut-off, there was no steam-pop on the QDOT side.
- ✓ All steam-pops on the DTA side occurred at 55℃ or higher.
- ✓ The higher the temperature of the DTA at the time of steam-pop, the deeper the cracks.